

# Multiphoton adaptation of a commercial low-cost confocal microscope for live tissue imaging

## James J. Mancuso

Baylor College of Medicine  
Verna and Marrs McLean Department of  
Biochemistry and Molecular Biology  
One Baylor Plaza  
Houston, Texas 77030

## Adam M. Larson

Baylor College of Medicine  
Department of Neuroscience  
One Baylor Plaza  
Houston, Texas 77030

## Theodore G. Wensel

Baylor College of Medicine  
Verna and Marrs McLean Department of  
Biochemistry and Molecular Biology  
and  
Department of Neuroscience  
One Baylor Plaza  
Houston, Texas 77030

## Peter Saggau

Baylor College of Medicine  
Department of Neuroscience  
One Baylor Plaza  
Houston, Texas 77030

## 1 Introduction

Multiphoton laser scanning microscopy (MPLSM) has emerged as a powerful tool in physiological imaging of live tissues. The use of long excitation wavelengths (700–1000 nm) results in reduced autofluorescence of biological tissue and significantly less light scattering.<sup>1</sup> In studies involving imaging of living brain tissues, these properties allow high-resolution imaging of fine structures, such as dendrites and even dendritic spines, with deep sample penetration by light.<sup>2</sup> In addition, by confining fluorescence excitation to a very small volume, multiphoton imaging eliminates photodamage out of the focal plane, allowing for long-term functional imaging experiments, such as monitoring of Ca<sup>2+</sup> transients in dendritic spines.<sup>3</sup>

Typically, those wishing to perform MPLSM have been left with the option of purchasing an off-the-shelf commercial system or building a “do-it-yourself” custom system utilizing an existing confocal scan head.<sup>4–6</sup> Often more affordable and flexible, custom-built systems have required a level of technical expertise and programming beyond that of a typical biologist. Additionally, even after design, assembly, and testing by an experienced optical engineer, these setups almost always require constant surveillance and tweaking by the original de-

**Abstract.** The Nikon C1 confocal laser scanning microscope is a relatively inexpensive and user-friendly instrument. We describe a straightforward method to convert the C1 for multiphoton microscopy utilizing direct coupling of a femtosecond near-infrared laser into the scan head and fiber optic transmission of emission light to the three-channel detector box. Our adapted system can be rapidly switched between confocal and multiphoton mode, requires no modification to the original system, and uses only a few custom-made parts. The entire system, including scan mirrors and detector box, remain under the control of the user-friendly Nikon EZ-C1 software without modification. © 2009 Society of Photo-Optical Instrumentation Engineers. [DOI: 10.1117/1.3139850]

Keywords: microscopy; multiphoton processes; confocal optics; pulsed laser; fiber coupled detection; instrumentation.

Paper 08434LR received Dec. 10, 2008; revised manuscript received Mar. 11, 2009; accepted for publication Mar. 28, 2009; published online May 27, 2009.

signer and are prone to software glitches. The presented system can be assembled, maintained, and utilized by any microscopists requiring multiphoton imaging capability.

## 2 Materials and Methods

A schematic of the converted system is shown in Fig. 1(a). We have directly coupled a femtosecond pulsed near-infrared (NIR) laser (Chameleon, Coherent) to the scan head to provide multiphoton excitation. The beam diameter is expanded to overfill the back focal aperture (BFA) of the objective lens, which eliminates any discrepancies arising from ellipticity of the excitation beam. The expanded beam is directed into the scan head (C1, Nikon) using a mirror insert (C50299, Nikon) equipped with a silver-surface full mirror (21010, Chroma) to replace the dichroic mirror insert employed in the original confocal configuration [inset of Fig. 1(a)]. The external optics (Microbench, Linos) consist of an adjustable neutral density filter wheel (5215, New Focus) that attenuates the beam, a 3× beam expander, and a beam aligner that directs the attenuated and expanded beam into the scan head through the mirror insert. All external optics are connected to the scan head through a custom-made adapter plate that bolts directly to the scan head after removal of the plastic clam-shell case utilizing existing clearance holes. The design of the adapter plate permits easy access to the mirror insert, which must be ex-

Address all correspondence to Peter Saggau, Baylor College of Medicine, Department of Neuroscience, One Baylor Plaza, Houston, TX 77030. Tel: 713-798-5082; E-mail: psaggau@bcm.edu

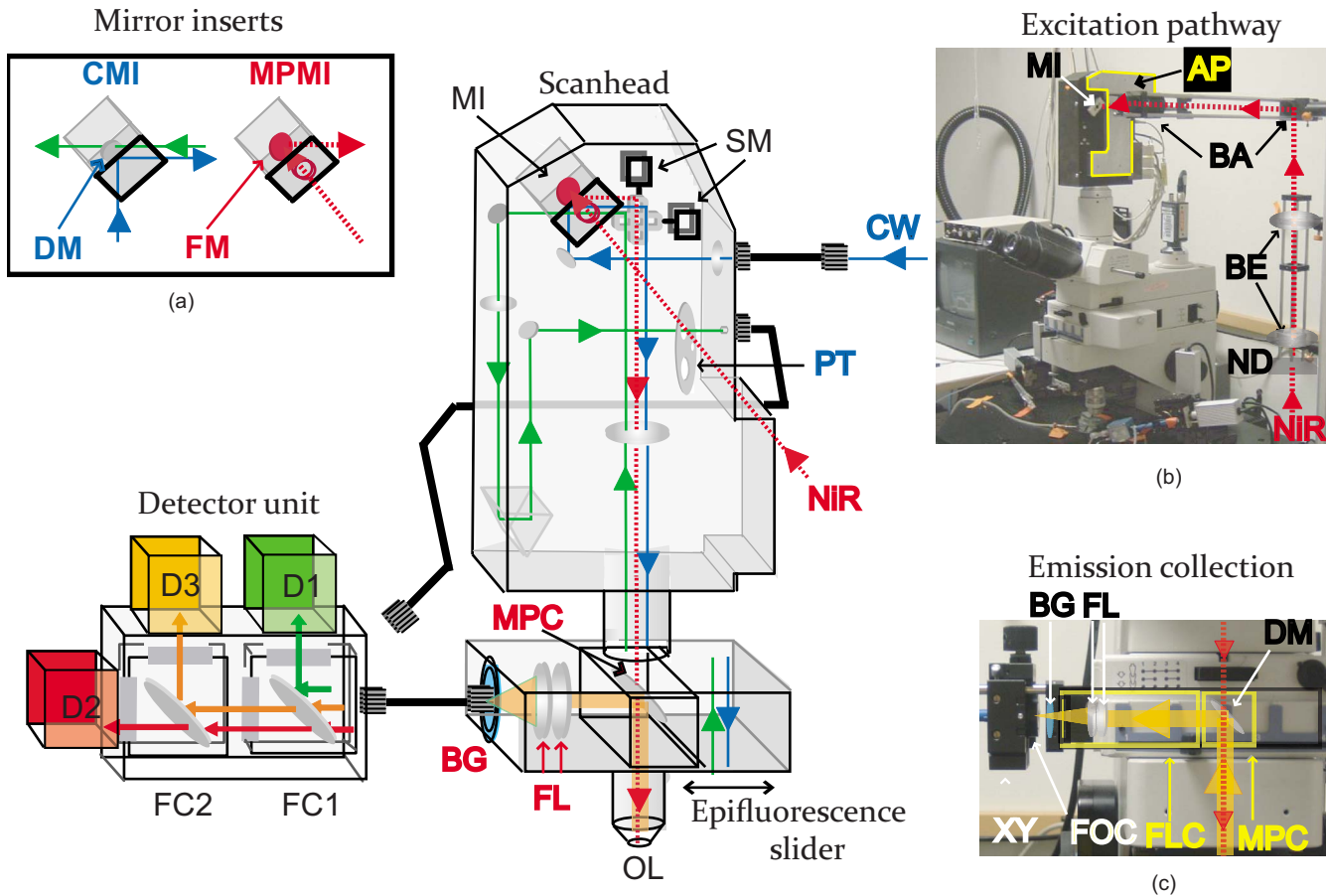


**Fig. 1** Confocal to multiphoton conversion. (a) Schematic of system adaptation. The near infrared (NIR) excitation path is shown in red, multiphoton-excited emission in orange, continuous wave (CW) excitation in blue, and standard single-photon-excited emission in green. Components utilized in both configurations are labeled in black, in only confocal in blue, and in only multiphoton in red. The setup is shown in the multiphoton configuration, where the detector unit is connected by multimode fiber optic cable to the epifluorescence slider and not the scan head. Abbreviations: mirror insert (MI), scan mirrors (SM), pinhole turret (PT), multiphoton cube (MPC), focusing lens (FL), blue glass filter (BG), objective lens (OL). Inset: Confocal mirror insert (CMI) using dichroic mirror (DM), multiphoton mirror insert (MPMI) using full mirror (FM). Detector unit: emission filter cubes (FC1,2), and PMT detectors (D1,2,3). (b) Multiphoton excitation pathway with NIR beam-passing neutral density filter (ND), telescoping beam expander (BE) consisting of 50- and 150-mm focal length achromats, and beam aligner (BA) before entering custom-made mirror insert (MI). Also shown is the custom-made adapter plate (AP) (highlighted in yellow) connecting the scan head to the external optics. (c) Multiphoton epi-fluorescence emission pathway. Two special cubes were connected to the rail inside the slider by means of its dovetail and clamping screws: A custom-made focusing cube (FLC, highlighted in yellow) was secured to the leftmost (as shown) part of the rail. This cube contains the 24-mm focal length lens combination (FL) and the 25-mm-diam tube that serves to anchor the microbench parts holding the BG39 emission filter, (BG), X-Y positioner (XY), and fiberoptic coupling (FOC). The custom-made MPC (highlighted in yellow) containing the DM is oriented such that the collected fluorescence is directed away from the scan head and toward the external detector unit, is then fastened to the same rail immediately adjacent to the focusing cube. The slider is placed in position 2 (as shown) for multiphoton microscopy and position 1 to remove the DM from the beam path in confocal mode. (Color online only.)

changed for switching between multiphoton and confocal modes [Fig. 1(b)]. The original C1 scan mirrors direct the excitation beam to the objective lens (e.g., 40 $\times$  water immersion, Fluor, Nikon). The BFA of this lens receives  $\sim 85\%$  of the laser power entering the scan head, as directly measured by a power meter (Lasermate 1, Coherent). In order to determine the effect of group velocity dispersion in our system, we measured the pulse length at the focal plane by interferometric autocorrelation (MINI Special, APE). All measurements were subjected to a low-pass filter and are the average of at least four measurements. The full width half maximum (FWHM) before the neutral density filter and after the scan head were 204 and 246 fs, respectively. This 25% increase in pulse length shows that the silver mirrors included in the scan

head are appropriate for multiphoton scanning.

In order to explore the feasibility of using an automated mechanism to modulate beam intensity, we inserted a 2-mm aperture acousto-optic deflector (AOD) (LS55, Isomet) into the unexpanded beam path, which increased the measured pulse length after the scan head by 30% to 318 fs. Spatial dispersion introduced by the AOD can be compensated by substituting a diffraction grating for one of the full mirrors in the beam path.<sup>7</sup> The expected 30% loss in laser power is of no consequence for *in vitro* imaging because all presented samples are imaged with a neutral density filter of at least optical density OD 1.5. The AOD can be controlled using the Nikon EZ-C1 software (Version 2.1) by connecting the C1

sync on the back of the C1 controller to an analog to digital converter (PCI-6035e, National Instruments).

Because of the highly local excitation volume, multiphoton imaging does not require spatial filtering by a confocal pinhole.<sup>8–10</sup> Therefore, multiphoton-excited epifluorescence is not returned to the scan head for descanning and spatial filtering by the pinhole, but rather is directly detected. The collection optics are located as close to the BFA of the objective as possible to maximize collection efficiency. For this purpose, an epifluorescence slider (Y-FL, Nikon) was added to the microscope, equipped with a custom filter cube (MPC) holding a long-pass dichroic mirror (770dxcx, Chroma) to direct the collected fluorescence away from the scan head and toward the external detector unit [Fig. 1(c)]. This design allows convenient switching between the multiphoton detection pathway and the original confocal configuration. Most importantly, no modification to the C1 scanhead or the epifluorescence slider is needed. Collected fluorescence is sent through a focusing cube (FLC) containing two sequentially placed visible corrected achromats of 35-mm focal length. This previously described lens system transmits >70% of the collected epifluorescence<sup>11</sup> through an infrared blocking filter (BG39, Schott) into a multimode fiberoptic cable (1.5 mm aperture, NA=0.39, ThorLabs). We mounted the optical cable through a 25-mm subminiature connector A (SMA) connector on an X-Y positioner (Microbench, Linos), which slides as shown on microbench rails along the Z-axis to allow easy adjustment for maximum transmission of emission light. For potential uncaging experiments, which require shorter excitation wavelengths, the 770-nm long-pass dichroic (Fig. 1, MPC) can be easily substituted with a dichroic mirror of shorter wavelength.

We connected the fiberoptic cable to the original detection unit of the C1 confocal microscope, containing three photomultiplier tubes (PMT) through its SMA connector. Use of the C1 detection unit allows for easy adaptation for various fluorophore combinations due to its exchangeable modular filter cubes.

Imaging can be performed using the standard imaging software (EZ-C1) provided with the confocal system, without modification to operate the scan mirrors, axial positioning of the objective lens, and PMT parameters. Wavelength and emission of the NIR laser can be controlled either directly on the front panel of the laser power supply or using the provided software interface (Chameleon, Coherent).

Images were processed using both the Nikon EZ-C1 software as well as ImageJ software, freely available through NIH. For point-spread function (PSF) approximation, a 3-D stack of images of a subresolution diameter fluorescent bead was acquired, and intensity values measured along a single axis were plotted versus distance and fit to a Gaussian distribution (Origin 6.0, Microcal). Exact technical specifications of custom-made parts are available on request.

### 3 Results

In order to evaluate the two-photon performance of the modified microscope, we chose to image different types of fluorescently labeled pollen grains (30-4264, Carolina Biological Supply), producing optical sections at 2- $\mu\text{m}$  axial steps.

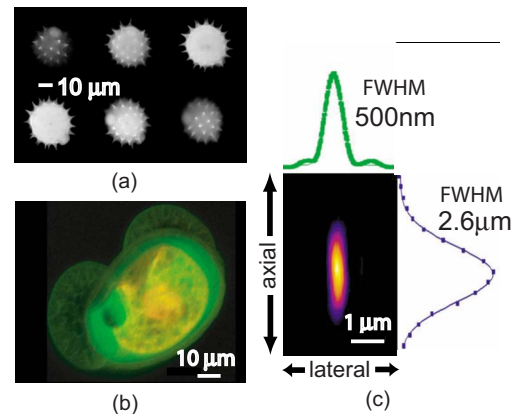


**Fig. 2** Two-photon performance of modified microscope. (a) 6- $\mu\text{m}$  optical sections of two-photon excited fluorescence from an Alexa 488 labeled pollen grain. (b) Maximum projection image constructed from a stack of 1- $\mu\text{m}$  optical sections of two-photon excited fluorescence from a pollen grain labeled with Alexa 488 (green) and Alexa 594 (red). (c) False color image z-plane reconstruction made from two-photon images of a subresolution bead (180 nm, Alexa 488). Shown are intensity profiles for the x and z planes along with the FWHM of intensity. Not shown y-axis FWHM=460 nm. (Color online only.)

Figure 2(a) shows six consecutive optical sections taken from a green-labeled spiky grain, illustrating the imaging capability of the modified system. Figure 2(b) is a maximum projection image of another dual-labeled, lobular pollen grain, reconstructed from two-photon excited fluorescence gathered in the first (green) and second (red) emission channels. Next, in order to determine the two-photon resolution of our microscope, we imaged subresolution fluorescent beads (180 nm, Molecular Probes) mounted on poly-D-lysine-coated glass cover slips using an excitation wavelength of  $\lambda=840$  nm and an objective lens of NA=0.8 [Fig. 2(c)]. The FWHM fluorescence intensity in both axial and lateral planes was determined as an approximation of the PSF. The experimentally obtained value of  $\text{FWHM}_{\text{axial}}=2.6 \mu\text{m}$  is a good match to the theoretical value  $\text{FWHM}_{\text{axial}}=2 \mu\text{m}$ .<sup>12</sup> Because the diameter of the bead approaches half of the theoretical excitation PSF of  $\text{FWHM}_{\text{lateral}}(388.5 \text{ nm})$ , its effect on the observed image was taken into account. Convolution of our theoretical Gaussian PSF with a sphere of 180 nm diameter yields a theoretical image of just over 400 nm FWHM in the lateral plane, comparable to our measured  $\text{FWHM}_{\text{lateral}}$  of 500 and 460 nm.

Finally, to demonstrate the effectiveness of the modified microscope for imaging of live tissue, we imaged mouse neuronal tissue. For structural imaging, whole retinas were extracted from heterozygous knock-in mice expressing a human rhodopsin-EGFP (enhanced green fluorescent protein) fusion protein.<sup>13</sup> The tissue was imaged in artificial cerebrospinal fluid with a  $512 \times 512$ -pixel scan pattern and a 2.6- $\mu\text{s}$  pixel dwell time. The excitation power at the BFA of a  $40\times$  (NA=0.8) water immersion objective lens (Fluor, Nikon) was  $\sim 30$  mW at 840 nm [Fig. 3(a)]. The images reveal fluorescence in clearly observable individual photoreceptor cell outer segments (1.4  $\mu\text{m}$  diam), where the rhodopsin protein localizes, which corresponds nicely to similar images taken on the

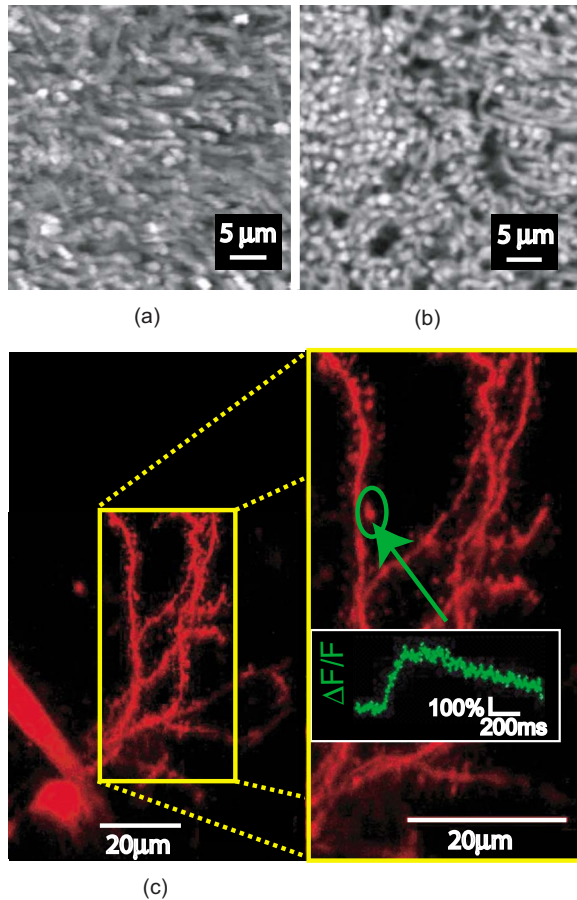


**Fig. 3** (a) Maximum projection of two-photon fluorescence images of a single Rhodopsin-EGFP expressing retina taken in multiphoton mode with no spatial filtering. (b) Maximum projection of single-photon fluorescence images of a single Rhodopsin-EGFP expressing retina taken in confocal mode and filtered through the 30- $\mu\text{m}$  (smallest) pinhole. (c) Two-photon images using a 100 $\times$  water immersion objective (NA=1.1) of a mouse striatal neuron in a brain slice filled with Alexa 594 and OGB-1. Inset is a 2 $\times$  zoom of the area bounded by the yellow box. The graph is the normalized change in OGB-1 fluorescence ( $\Delta F/F$ ) in the circled dendritic spine in response to a train of action potentials, measured in line-scan mode. (Color online only.)

C1 using the confocal configuration [Fig. 3(b)] with the smallest pinhole (30  $\mu\text{m}$ ).

In order to demonstrate the capacity to conduct functional imaging experiments, striatal brain slices were prepared from C57 mice. Individual neurons were whole-cell patched and dialyzed with a standard internal solution containing 200  $\mu\text{M}$  of the fluorescent calcium indicator dye Oregon Green BAPTA-1 (OGB-1) and 50  $\mu\text{M}$  of the fluorescent label Alexa Fluor 594. Imaging was performed using a 100 $\times$  (NA = 1.1) water immersion objective (Plan, Nikon) and  $\sim 12\text{-mW}$  BFA average power at 810-nm excitation. Dendritic structures of a striatal spiny neuron are presented in Fig. 3(c) as a maximum projection image generated from a series of optical sections separated by 0.5  $\mu\text{m}$ . During functional imaging, a train of 15 action potentials was induced by injecting depolarizing current into the soma in current clamp mode. Calcium influx was determined as the increase of OGB-1 fluorescence normalized by its resting fluorescence ( $\Delta F/F$ )

throughout the course of a line scan through a single spine [Fig. 3(c) inset]. No significant bleaching or obvious photo-damage was observed throughout the course of imaging. The low laser power used as well as the good signal-to-noise ratio of the  $\text{Ca}^{2+}$  signal observed from easily discernible distal dendritic spines illustrate that our modified laser scanning microscope can be used effectively for functional imaging experiments with multiphoton excitation.

## 4 Conclusion

We have presented a straightforward and effective multiphoton adaptation of a common commercial confocal microscope that allows rapid switching between confocal and multiphoton modes. The entire conversion requires no modification of the original system and only a few custom-made parts. The previously demonstrated efficient fiber optic coupling of epifluorescence emission<sup>11</sup> to the C1 detection unit allows for convenient simultaneous probing of multiple fluorophores that can quickly be changed using the modular filter cubes present in this unit. The imaging software of the original confocal system can be used without any modifications for multiphoton imaging.

The presented microscope is ideal for biological imaging applications with limited sample depth and short-term functional imaging and could be modified by users with little or no mechanical or electronics experience. Control of acousto-optic modulation as presented makes possible further improvements, including modulation of laser power with sample depth, blanking the beam during the backscan (which reduces exposure time by up to 56%), fast modulation of laser intensity for fluorescence recovery after photobleaching (FRAP) experiments, and coupling uncaging with functional imaging.

Except for the pulsed NIR laser, the components used are relatively inexpensive and widely available. We have demonstrated the system's utility by imaging fluorescent proteins and indicator dyes of a number of different excitation and emission wavelengths in two different neuronal preparations. This versatile microscope can be utilized by groups that lack either the resources to purchase a prepackaged system or the technical know-how to build a new system from scratch.

## Acknowledgments

The presented work was supported by NIH training grant No. EY T32 EY07102 (J.J.M.), NIH Grants No. R01-EY11900 and No. R01-DA015189, and Welch Foundation Grant No. Q0035 (T.G.W.) as well as Grants No. NIH-NIA/RO1 AG027577 and No. NSF/DBI-0455905 (P.S.).

## References

1. W. Denk, J. H. Strickler, and W. W. Webb, "2-Photon laser scanning fluorescence microscopy," *Science* **248**(4951), 73–76 (1990).
2. K. Svoboda and R. Yasuda, "Principles of two-photon excitation microscopy and its applications to neuroscience," *Neuron* **50**(6), 823–839 (2006).
3. W. Denk, R. Yuste, K. Svoboda, and D. W. Tank, "Imaging calcium dynamics in dendritic spines," *Curr. Opin. Neurobiol.* **6**(3), 372–378 (1996).
4. A. Majeswska, G. Yiu, and R. Yuste, "A custom-made two-photon microscope and deconvolution system," *Pflugers Arch. Eur. J. Physiol.* **441**(2–3), 398–408 (2000).

5. C. Soeller and M. B. Cannell, "Construction of a two-photon microscope and optimisation of illumination pulse duration," *Pfluegers Arch. Eur. J. Physiol.* **432**(3), 555–561 (1996).
6. A. Ridsdale, I. Micu, and P. K. Stys, "Conversion of the Nikon C1 confocal laser-scanning head for multiphoton excitation on an upright microscope," *Appl. Opt.* **43**(8), 1669–1675 (2004).
7. V. Iyer, B. E. Losavio, and P. Saggau, "Compensation of spatial and temporal dispersion for acousto-optic multiphoton laser-scanning microscopy," *J. Biomed. Opt.* **8**(3), 460–471 (2003).
8. D. W. Piston, E. S. Wu, and W. W. Webb, "3-Dimensional diffusion measurements in cells by 2-photon excitation fluorescence photobleaching recovery," *FASEB J.* **6**(1), A34 (1992).
9. D. W. Piston, M. S. Kirby, H. P. Cheng, W. J. Lederer, and W. W. Webb, "2-Photon-excitation fluorescence imaging of 3-dimensional calcium-ion activity," *Appl. Opt.* **33**(4), 662–669 (1994).
10. W. Denk and P. B. Detwiler, "Optical recording of light-evoked calcium signals in the functionally intact retina," *Proc. Natl. Acad. Sci. U.S.A.* **96**(12), 7035–7040 (1999).
11. A. Larson, V. Iyer, T. Hoogland, and P. Saggau, "Fiber-coupled non-descanned 4 pi detection with a commercial confocal microscope modified for multiphoton imaging," *Proc. SPIE* **4963**(1), 239–251 (2003).
12. R. M. Williams, D. W. Piston, and W. W. Webb, "2-Photon molecular-excitation provides intrinsic 3-dimensional resolution for laser-based microscopy and microphotochemistry," *FASEB J.* **8**(11), 804–813 (1994).
13. F. Chan, A. Bradley, T. G. Wensel, and J. H. Wilson, "Knock-in human rhodopsin-GFP fusions as mouse models for human disease and targets for gene therapy," *Proc. Natl. Acad. Sci. U.S.A.* **101**(24), 9109–9114 (2004).